

## SPLINE METHODS FOR CONSERVATION EQUATIONS

C. Bottcher and M. R. Strayer  
Oak Ridge National Laboratory  
Oak Ridge, TN 37831-6373

## DISCLAIMER

This report was prepared as an account of work sponsored by an agency of the United States Government. Neither the United States Government nor any agency thereof, nor any of their employees, makes any warranty, express or implied, or assumes any legal liability or responsibility for the accuracy, completeness, or usefulness of any information, apparatus, product, or process disclosed, or represents that its use would not infringe privately owned rights. Reference herein to any specific commercial product, process, or service by trade name, trademark, manufacturer, or otherwise does not necessarily constitute or imply its endorsement, recommendation, or favoring by the United States Government or any agency thereof. The views and opinions of authors expressed herein do not necessarily state or reflect those of the United States Government or any agency thereof.

to be published in

Proceedings of

*Third IMACS Symposium on Computational Acoustics*  
Cambridge, Massachusetts  
June 26-28, 1991

MASTER

"The submitted manuscript has been authored by a contractor of the U.S. Government under contract No. DE-AC05-84OR21400. Accordingly, the U.S. Government retains a nonexclusive, royalty-free license to publish or reproduce the published form of this contribution, or allow others to do so, for U.S. Government purposes."

*ds*  
DISTRIBUTION OF THIS DOCUMENT IS UNLIMITED

# SPLINE METHODS FOR CONSERVATION EQUATIONS

C. Bottcher and M. R. Strayer

*Center for Computationally Intensive Physics*

*Physics Division, Oak Ridge National Laboratory*

*Oak Ridge, TN 37831*

## Abstract

We consider the numerical solution of physical theories, in particular hydrodynamics, which can be formulated as systems of conservation laws. To this end we briefly describe the Basis Spline and Collocation methods, paying particular attention to representation theory, which provides discrete analogues of the continuum conservation and dispersion relations, and hence a rigorous understanding of errors and instabilities. On this foundation we propose an algorithm for hydrodynamic problems in which most linear and nonlinear instabilities are brought under control. Numerical examples are presented from one-dimensional relativistic hydrodynamics.

## 1. THE CONSERVATION LAWS OF THEORETICAL PHYSICS

It has long been recognised that the partial differential equations of theoretical physics are advantageously cast in the form of conservations laws <sup>1)</sup>. This is particularly true of hydrodynamics, as for more general transport problems, where the equations express the conservation of energy, momentum, entropy and so forth. If the conservation theorems can be preserved in a numerical solution, instabilities and errors are thereby controlled to some degree. Most classic discussions of stability are based on conserving energy, which may be sufficient in simple problems. In general, conservation is a necessary, but not sufficient condition, for stability, particularly in nonlinear problems. A more complete set of criteria is presented below.

Suppose a system is described by  $N_c$  conserved quantities  $\{\phi_K(\vec{r})\}$ . Evolution in time must be governed by equations of the form

$$\frac{\partial \phi_K}{\partial t} = -\nabla \cdot \vec{F}_K[\phi] + S_K, \quad K = 1, \dots, N_c. \quad (1)$$

The integral-conserved quantities, such as the total mass, are given by

$$Q_K = \int d^3r \phi_K, \quad (2)$$

and satisfy

$$\frac{dQ_K}{dt} = \int d^3r S_K. \quad (3)$$

If the source term  $S_K$  is zero,  $Q_K$  is constant. We suppose that the equations are solved in an infinite domain, in which the generalized currents  $\vec{F}_K$  vanish at

large distances faster than  $r^{-2}$ . The equations (1) are closed by making the  $\vec{F}_K$  functions or functionals, in general nonlinear, of the left hand  $\phi_K$ .

All discretizations of (1) seek to replace the continuous functions  $\{\phi_K(\vec{r})\}$  by vectors  $\phi_K$ , and the operators  $\partial/\partial x_a$  by matrices  $D_a$ , where  $a = 1, 2, 3$  ( $x, y, z$ ).

The resulting equations,

$$\frac{\partial \phi_K}{\partial t} = - \sum_{a=1}^3 D_a F_{K_a}[\phi] + S_K, \quad (4)$$

retain a discrete form of the conservation laws if it is possible to find a vector  $\omega$  such that

$$\omega^\dagger D_a = 0. \quad (5)$$

The integral-conserved quantities are

$$Q_K = \omega^\dagger \phi_K, \quad (6)$$

so that the elements of  $\omega$  play the role of quadrature weights <sup>2)</sup>.

Specific examples of equations which can be cast in the form (1) are nonrelativistic hydrodynamics <sup>3)</sup>, for which

$$\phi = \begin{bmatrix} \rho \\ \rho \vec{u} \end{bmatrix}, \quad \vec{F} = \begin{bmatrix} \rho \vec{u} \\ \rho \vec{u} \vec{u} + \Pi \end{bmatrix}, \quad (7)$$

where  $\rho$  is the density,  $\vec{u}$  the local velocity, and  $\Pi = \int P(\rho) d\rho/\rho$  the Riemann pressure. The generalization of (7) to special relativity is neither trivial nor unique, but we shall use the form due to Landau <sup>4)</sup>,

$$\phi = \epsilon u_0 \begin{bmatrix} u_0 \\ \vec{u} \end{bmatrix}, \quad \vec{F} = \begin{bmatrix} \vec{\phi} \\ \frac{\vec{\phi} \vec{\phi}}{\phi_0 + P} \end{bmatrix}, \quad (8)$$

where  $\epsilon$  is the energy density,  $u = (u_0, \vec{u})$  the local four-velocity, and  $P(\epsilon)$  the pressure. The energy density is derived from  $\phi$  by solving the nonlinear equation

$$\epsilon = \phi_0 - \frac{\vec{\phi}^2}{\phi_0 + P}. \quad (9)$$

Nuclear matter at high excitations, such as might be produced in collisions of heavy ions at relativistic energies, is believed to be described by equations of the type (8). While plans to study matter under these conditions in large accelerators are underway in the U.S.A. and Europe, theoretical progress has been slowed by the numerical intractability of most theories. Thus it is not known whether specific models predict shock waves, sideways flow or stopping. The present investigations are directed towards finding robust algorithms for solving (8) for the case of nuclear collisions. A detailed discussion of hydrodynamics as applied to relativistic nuclear collisions, with a bibliography, has been given by Gatoff *et al*<sup>5)</sup>.

## 2. THE BASIS SPLINE AND COLLOCATION METHODS

Splines of order  $\mathcal{N}$  are functions  $S^{\mathcal{N}}(x)$  of a single real variable belonging to the class  $C^{\mathcal{N}-2}$  with continuous  $(\mathcal{N} - 2)^{\text{th}}$  derivatives. Each spline is associated with a set of points  $\{x_k\}$ , called knots; we take the knots to be distinct and ordered,  $x_k < x_{k+1}$ . Between each pair of knots, the spline is a polynomial of degree  $\mathcal{N} - 1$  (the order refers to the number of coefficients); at each knot, the function

and derivatives up to the  $(\mathcal{N} - 2)^{\text{th}}$  are continuous. The  $(\mathcal{N} - 1)^{\text{th}}$  derivative is bounded but discontinuous. We shall consider only even orders  $\mathcal{N} \geq 3$ .

Splines have long been used for curve fitting, but the introduction of basis splines greatly enhanced the power of the technique by bringing to it the language of functional analysis. Given a set of knots  $\{x_k\}$ , the basis splines of order  $\mathcal{N}$  are a set of functions  $B_k^{\mathcal{N}}(x)$  such that any spline  $S^{\mathcal{N}}(x)$  is identically a linear superposition

$$S^{\mathcal{N}}(x) \equiv \sum_k a_k B_k^{\mathcal{N}}(x). \quad (10)$$

It is easy to see that  $B_k^{\mathcal{N}}(x)$  is uniquely defined by the condition that it is zero outside the range of  $\mathcal{N} + 1$  consecutive knots  $x_k, x_{k+1}, \dots, x_{k+\mathcal{N}}$ . Such a function of order  $\mathcal{N} = 3$  is illustrated in Fig. 1. At either end of the range of knots, the basis splines can be modified to incorporate boundary conditions. One can better visualize how splines are used by considering an example, as in Fig. 2, of a set of splines fitted together to represent functions satisfying some boundary conditions; in this case,

$$\psi(x_1) = 0, \quad \psi'(x_N) = 0, \quad (11)$$

where the prime denotes differentiation. Several algorithms are described in the literature to construct basis splines from the continuity conditions at the knots and the boundary conditions at the endpoints (6,7,2,8).

Given the basis splines, a function  $\psi(x)$  is approximated by the interpolant  $\hat{\psi}$ , where

$$\hat{\psi}(x) = \sum_{k=1}^N \psi^k B_k(x), \quad (12)$$

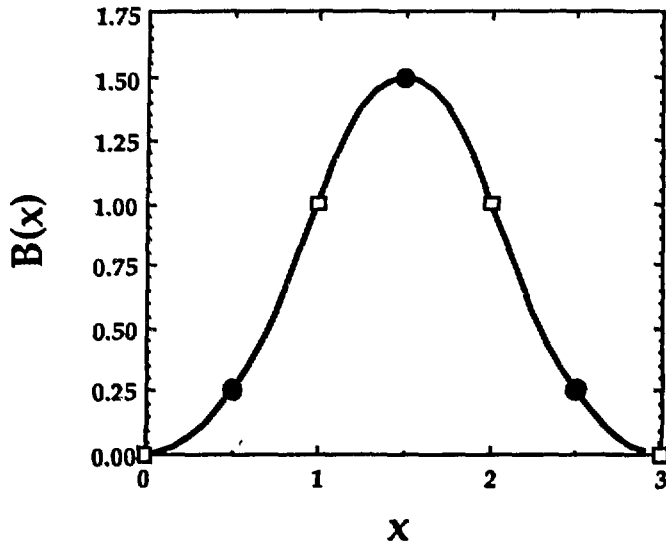


Fig. 1. Basis spline of order  $\mathcal{N} = 3$ . The knots are denoted by open squares, and the collocation points by filled circles.

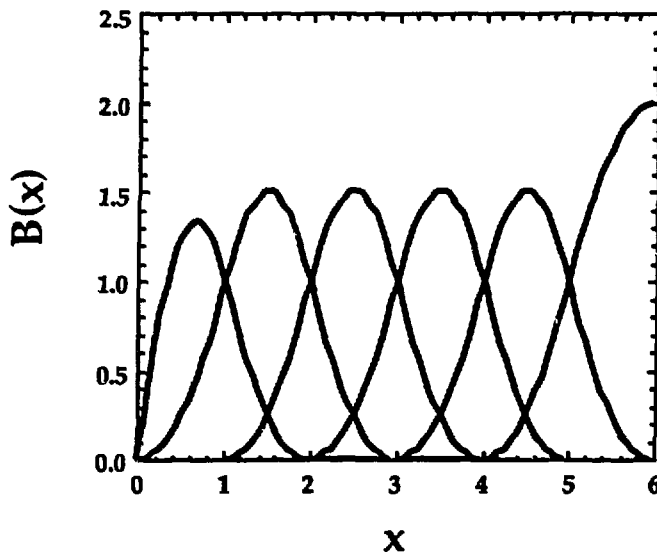


Fig. 2. Set of basis splines of order  $\mathcal{N} = 3$  satisfying the boundary conditions (11).

and the  $\psi^k$  are determined if  $\hat{\psi}(x) \equiv \psi(x)$  at a set of  $N$  data, or *collocation*, points  $\{\xi_\alpha\}$ . We have only to solve

$$\sum_{k=1}^N B_{\alpha k} \psi^k = \psi_\alpha, \quad (13)$$

where  $B_{\alpha k} = B_k(\xi_\alpha)$  and  $\psi_\alpha = \psi(\xi_\alpha)$ ; the order  $\mathcal{N}$  is omitted for simplicity. It is necessary and sufficient that the matrix  $\mathbf{B}$  be nonsingular: this will always be the case if we limit our considerations to odd orders and choose the collocation points halfway between the knots. Further, as is clearly seen in Fig. 1, the elements of  $\mathbf{B}$  are positive and largest on the diagonal, implying that the inversion of (13) is very stable. It is convenient to have a notation for the inverse of  $\mathbf{B}$ : we write the elements as  $B^{k\alpha}$  so that

$$\sum_{k=1}^N B^{k\alpha} \hat{\psi}^\alpha = \psi^k. \quad (14)$$

Formulae for derivatives and integrals are readily derived from (12)–(14) <sup>2)</sup>.

The collocation method for solution of an operator equation, formally written as

$$L[\psi] = 0, \quad (15)$$

is intimately related to the interpolation procedure of (12)–(14). We obtain  $N$  equations for the unknowns  $\{\psi^k\}$  by requiring that

$$L[\sum \psi^k B_k] = 0 \text{ at } x = \xi_\alpha. \quad (16)$$

Though the method is perfectly applicable to nonlinear problems, we are mostly concerned with linear operators  $L$ , in which case (16) becomes

$$\sum_{k=1}^N \psi^k L[B_k]_{x=\xi_\alpha} = 0 . \quad (17)$$

If we use (13) and (14) to eliminate the coefficients  $\{\psi^k\}$  in favour of the values of the solution  $\{\psi^k\}$  at the collocation points, (17) is replaced by

$$\sum_{\alpha=1}^N L_{\beta\alpha} \psi_\alpha = 0 , \quad (18)$$

where

$$L_{\beta\alpha} = \sum_{k=1}^N B^{k\alpha} L[B_k]_{x=\xi_\beta} = 0 .$$

As a simple example, consider a diffusion equation in one dimension,

$$\frac{\partial \psi}{\partial t} = \left[ \frac{d^2}{dx^2} - W(x) \right] \psi , \quad (19)$$

where  $W$  is a local sink term. An agreeable feature of the method is that expressions such as  $W\psi$  are replaced by  $W_\alpha \psi_\alpha$ , where  $W_\alpha = W(\xi_\alpha)$ . In other words, local operators come to be represented simply as diagonal matrices of their values at the collocation points. Nonlocal operators such as derivatives appear more complicated at first sight. In summary, (20) is replaced by

$$\frac{\partial \psi_\alpha}{\partial t} = \sum_{\beta=1}^N (\Delta_{\alpha\beta} - W_\alpha \delta_{\alpha\beta}) \psi_\beta , \quad (20)$$

where

$$\Delta_{\alpha\beta} = \sum_{k=1}^N B''_{\alpha k} B^{k\beta} , \quad B''_{\alpha k} = \left[ \frac{d^2 B_k}{dx^2} \right]_{x=\xi_\alpha} . \quad (21)$$

The analysis of (15)–(21) is readily extended to problems in two and three dimensions. Thus suppose (19) is written for three cartesian coordinates,

$$\frac{\partial \psi}{\partial t} = [\Delta^x + \Delta^y + \Delta^z - W(x)] \psi, \quad (22)$$

where  $\Delta^x = d^2/dx^2$  etc. The procedure of (12) is generalized by expanding the solution in products

$$\psi(x, y, z) = \sum_{ijk} \psi^{ijk} B^i(x) B^j(y) B^k(z). \quad (23)$$

For simplicity of exposition we assume that the same set of splines is associated with each coordinate. In collocation space we find that the representations of the operators analogous to those of (20) are given by

$$\begin{aligned} \Delta_{\alpha\beta\gamma, \alpha'\beta'\gamma'} &= \Delta_{\alpha, \alpha'}^x \delta_{\beta, \beta'} \delta_{\gamma, \gamma'} + \Delta_{\beta, \beta'}^y \delta_{\alpha, \alpha'} \delta_{\gamma, \gamma'} + \Delta_{\gamma, \gamma'}^z \delta_{\alpha, \alpha'} \delta_{\beta, \beta'} \\ W_{\alpha\beta\gamma, \alpha'\beta'\gamma'} &= W(\xi_\alpha, \xi_\beta, \xi_\gamma) \delta_{\alpha, \alpha'} \delta_{\beta, \beta'} \delta_{\gamma, \gamma'}. \end{aligned} \quad (24)$$

More detailed discussions of the basis-spline-collocation method, emphasizing quantum mechanical problems, is contained in the proceedings of a summer school held in Sewanee, Tennessee in 1989<sup>9)</sup>.

### 3. REPRESENTATION THEORY

In the most general sense, the title of this section includes all attempts to quantify the degree to which the discrete lattice representations derived in Section 2 accurately represent important features of the original problem. We will address the following features in particular: completeness, convergence, conservation laws and dispersion relations.

Given a formal interpolation procedure, such as that implied by (11)–(13), the issue of completeness refers to how well the interpolant  $\hat{\psi}(x)$  represents  $\psi(x)$  at

points other than the exactly fitted points  $\{\xi_\alpha\}$ . In other words, how does the error

$$\mathcal{E}(x) = |\psi(x) - \hat{\psi}(x)| \quad (25)$$

behave globally? A simple estimate is obtained from the Dirichlet functions  $B_k(x)$ , which arise when  $\hat{\psi}$  is expressed directly in terms of  $\{\psi_\alpha\}$ . From ((11)-(13), we find that

$$\hat{\psi}(x) = \sum_{k=1}^N \psi_\alpha \hat{B}_\alpha(x), \quad \hat{B}_\alpha(x) = \sum_{k=1}^N B^{k\alpha} R_k(x). \quad (26)$$

A typical Dirichlet function is shown in Fig. 3. It is evident that  $\hat{B}_\alpha(\xi_\beta) = \delta_{\alpha\beta}$  by construction, but at other points,  $\hat{B}_\alpha$  is nonzero and oscillating in sign. The values of  $|\hat{B}_\alpha|$  at successive turning points  $\xi'_\beta$  fall off rapidly; in fact, approximately as

$$0.3 \exp \left[ -\frac{(\xi_\alpha - \xi'_\beta)^2}{2N\Delta^2} \right],$$

for knots with a uniform spacing  $\Delta^2$ ). At the first minimum, however,  $\hat{B}_\alpha \simeq -0.3$ .

Thus the maximum of the error function (25) is estimated to be

$$\mathcal{E}_{\max} \simeq 0.3 \max_\alpha |\psi_{\alpha+1} - \psi_\alpha|. \quad (27)$$

The largest error is encountered if  $\psi$  has a discontinuity, as for a step function. However, in virtue of the rapid rate of falling off of  $\hat{B}_\alpha(x)$  with  $|x - \xi_\alpha|$ , the overshooting oscillations in the fit also die off rapidly with distance from the discontinuity. This contrasts with the notorious behaviour of Fourier or orthogonal polynomial interpolation.

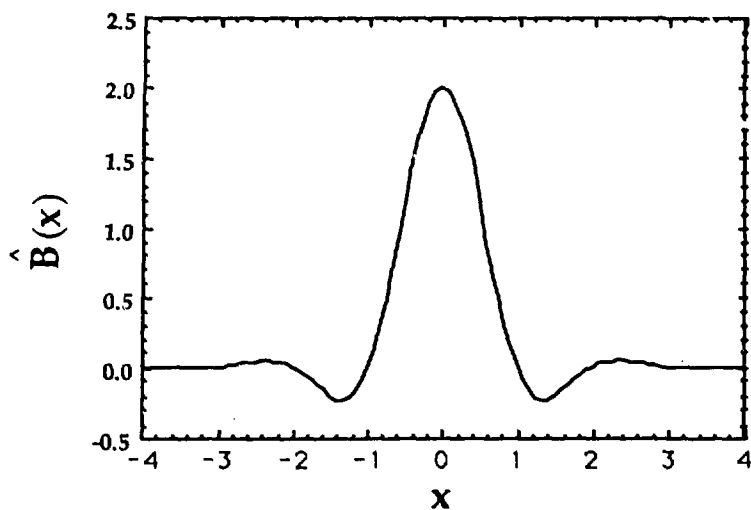


Fig. 3. Dirichlet function for basis splines of order  $\mathcal{N} = 3$ , as defined by (26).

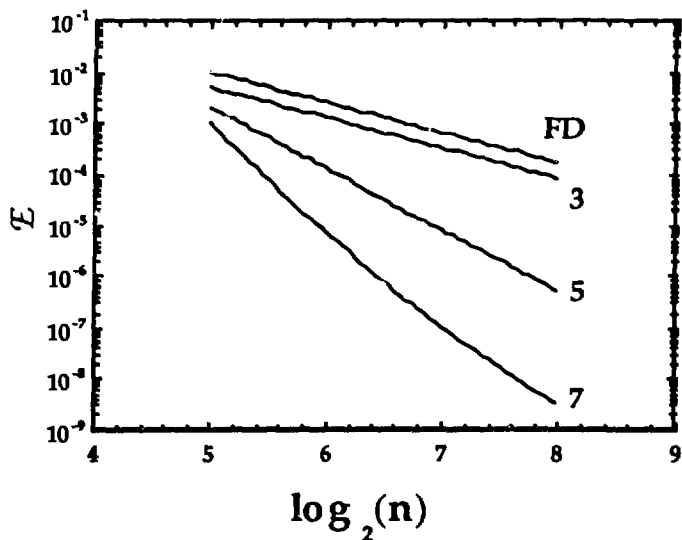


Fig. 4. Errors in the lowest eigenvalue of a Morse potential vs. the number of grid points  $n$  for different discretization algorithms. Reading from the top down, the curves refer to the three-point finite difference method, and the basis-spline-collocation method with splines of orders 3, 5 and 7 respectively. The model is described in more detail in Ref. 2).

When splines are used to fit smooth functions (of class  $C^M$  where  $M > 1$ , say), the solutions to operator problems usually converge uniformly as the number of points is increased. A point of great practical significance is that the rate of convergence improves as the order of the splines increases: usually  $\mathcal{E} \sim \Delta^{-\mathcal{N}+1}$ . This is illustrated by Fig. 5 which shows the errors in the lowest eigenvalue of the Schrödinger equation for a Morse potential <sup>2)</sup>. Usually  $\mathcal{N} = 7$  is adequate for practical purposes. Though spline interpolation remains stable for any order, a trend of diminishing returns is usually observed for  $\mathcal{N} > 9$ ; for increasing  $\mathcal{N}$  more splines may be needed to accommodate the boundary conditions instead of representing the solution.

The concept of a *faithful* representation of a differential operator is taken over from the mathematical literature <sup>6)</sup>. For our purposes, it means that the representation faithfully simulates the familiar intuitive properties of the differential calculus. No approximation can reproduce all properties exactly, but we can base our development on the following choice. Given the operator  $D = d/dx$ , we require that its matrix representation  $\mathbf{D}$  satisfies a subset of identities

$$\mathbf{D}\chi_M = \chi_{M-1}, \quad (28)$$

analogous to those for differentiating the monomials

$$\chi_M(x) = \frac{x^M}{M!}. \quad (29)$$

Insofar as the basis splines belong to the class  $C^{\mathcal{N}-2}$ , (28) holds identically for  $M \leq \mathcal{N} - 2$ . In general, the identity is modified near the boundaries where the

polynomial representation is modified to represent the boundary conditions.

For the simplest case of periodic boundary conditions, the representation satisfies an identity of the form (28),

$$\mathbf{D}\chi_0 = 0, \quad (30)$$

where  $\chi_{0\alpha} = 1 \forall \alpha$ . In general  $\chi$  is the eigenvector of  $\mathbf{D}$  corresponding to a zero eigenvalue. The accompanying right hand eigenvector  $\omega_0$  defines a set of quadrature weights in accordance with the prescription (5), providing  $\omega_0$  is appropriately normalized. The significance of (5) is seen by applying both sides to an arbitrary vector  $\psi$ , which recovers the familiar formula for the integral of a derivative. This in turn leads to an analogue of Green's lemma as an identity on the lattice, and finally to exact conservation laws on the lattice<sup>2)</sup>, as indicated in Section 1.

We use the term *dispersion* to refer to departures from the idealized propagation of a wavepacket described by

$$\frac{\partial \psi}{\partial t} = -\frac{\partial \psi}{\partial x}, \quad (31)$$

due to errors in the discrete realization

$$\frac{\partial \psi}{\partial t} = -\mathbf{D}\psi. \quad (32)$$

For uniformly spaced points and periodic boundary conditions on an interval  $-L \leq x \leq L$ , the behaviour of (32) is readily analysed. The solution can be expanded in eigenvectors of  $\mathbf{D}$ , given by  $\mathbf{D}\chi_n = \omega_n\chi_n$ . The eigenvectors have components  $\chi_{n\alpha} = \exp(-ik_n\xi_\alpha)$ , where the wavenumbers  $k_n = n\pi/L$ . Then solutions of (32) assume the form

$$\psi_\alpha = \sum_n a_n \chi_{\alpha n} \exp\{ik_n[\mathcal{D}(k_n)t - \xi_\alpha]\}, \quad (33)$$

where dispersion is characterized by departures from unity of the function  $\mathcal{D}(k_n) = \omega_n/k_n$ . Figure 5 shows  $\mathcal{D}$  as a function of  $q = k/k_{\max}$  for splines of order 3, 5 and 9. For  $q > \frac{1}{2}$ , all representations fail, but for smaller values, higher orders are far superior. In summary, splines of high order, say  $> 5$ , correctly describe dispersion down to wavelengths corresponding to two or three mesh spacings.

#### 4. APPLICATION TO HYDRODYNAMICS

As an example, we consider relativistic hydrodynamics described by the system of equations (4), (7) and (8) in one space dimension. At the outset we have to recognize that no complete theory is available for the numerical solution of hydrodynamic problems. The difficulties peculiar to each case must be considered on their merits. Relativistic problems have special difficulties due to the existence of multiple scales and shocks. The desirable criteria which the solutions should satisfy are:

- The conservation laws are recovered.
- Dispersion is minimized.
- Maximal theorems (see (39) below) are preserved.
- Nonlinear instabilities are controlled.

We propose an algorithm incorporating the following features, which will then be discussed in more detail. A detailed description of of this algorithm, including

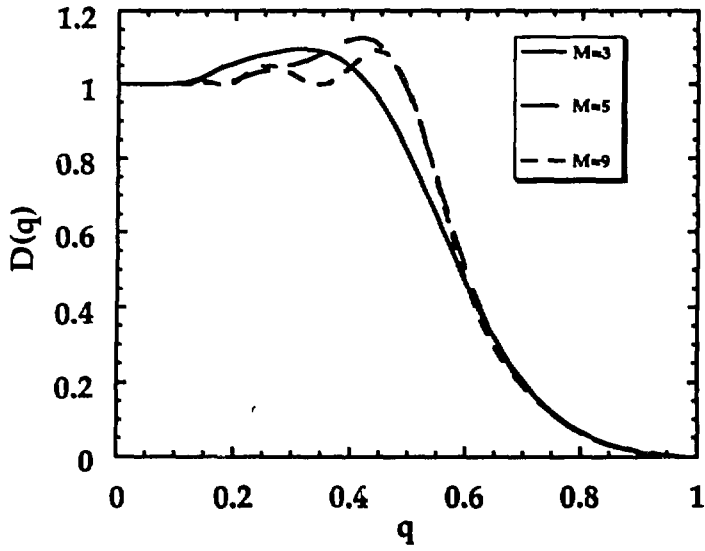


Fig. 5. Dispersion function for basis splines of order  $N = 3, 5, 9$ , as defined by (33).

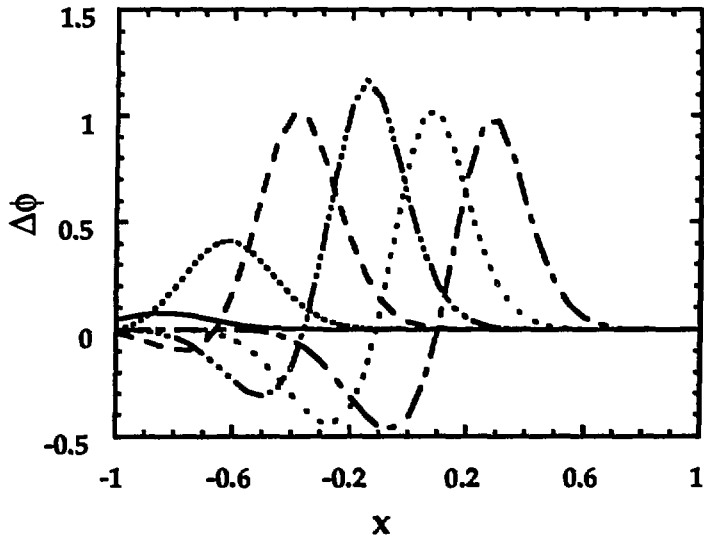


Fig. 6. Propagation of nonlinear noise, as described by (41).

proofs of results merely stated here, will be given in a forthcoming publication.

- The solution is discretized using high order splines.
- Propagation from one timestep to the next is performed by a nonlinear mapping, which is iteratively corrected.
- The mapping incorporates hopscotch averaging.
- An artificial viscosity is introduced.

By using high order splines, we take care of the conservation laws and dispersion relations, as described in Section 3.

The time propagation is achieved by introducing a nonlinear mapping. If the equations are written in shorthand as

$$\frac{\partial \phi}{\partial t} = \mathcal{F}[\phi], \quad (34)$$

the solutions at  $t, t + \tau$  are related by

$$\phi_{t+\tau} - \phi_t = \tau \mathcal{F}[\text{avg}(\phi_{t+\tau}, \phi_t)] + \mathcal{O}(\tau^3), \quad (35)$$

where the last term indicates the error. The average is defined in general by a relation of the form (where  $m$  labels time and  $\alpha$  space)

$$\text{avg}(\phi_{m+1}^\alpha, \phi_m^\alpha) = \theta_m^\alpha \phi_{m+1}^\alpha + (1 - \theta_m^\alpha) \phi_m^\alpha. \quad (36)$$

“Hopscotch” averaging divides the lattice into odd and even points, and sets

$$\theta_m^\alpha = \delta(m + \alpha, \text{even}). \quad (37)$$

In two or three dimensions, a checkerboard pattern is used. This scheme damps out instabilities in which the odd and even points propagate independently. Our method hinges on iterating (35) until the residuals fall below a prescribed threshold, usually  $10^{-6}$ . This is the primary control of nonlinear noise. It can be proved that the iteration converges to the correct answer providing the timestep is small enough (but finite),

$$\tau \max \|\mathcal{F}\| \leq \theta < 1. \quad (38)$$

Under this condition, it can be shown further that the maximal theorems are preserved from one step to the next. These are, for the system under consideration,

$$\phi_0 \geq 0, \quad \phi_0^2 - \bar{\phi}^2 \geq 0, \quad (39)$$

corresponding respectively to the positivity of the density and causality.

Having taken all the precautions just described, solutions are still plagued by high-frequency instabilities. Though their appearance can be postponed to late in the time evolution, it seems to be inevitable. The source of these persistent instabilities appears to be the amplification of random noise by nonlinear mode coupling. The power spectrum

$$A(k) = \left| \int_{-\infty}^{\infty} dk \phi(x) \exp(-ikx) \right|^2 \quad (40)$$

is a convenient diagnostic of this phenomenon. If we consider a model problem with mode coupling

$$\frac{\partial \phi}{\partial t} = -\frac{\partial}{\partial x}(u[\phi]\phi) - \nu \frac{\partial^2 \phi}{\partial x^2}, \quad (41)$$

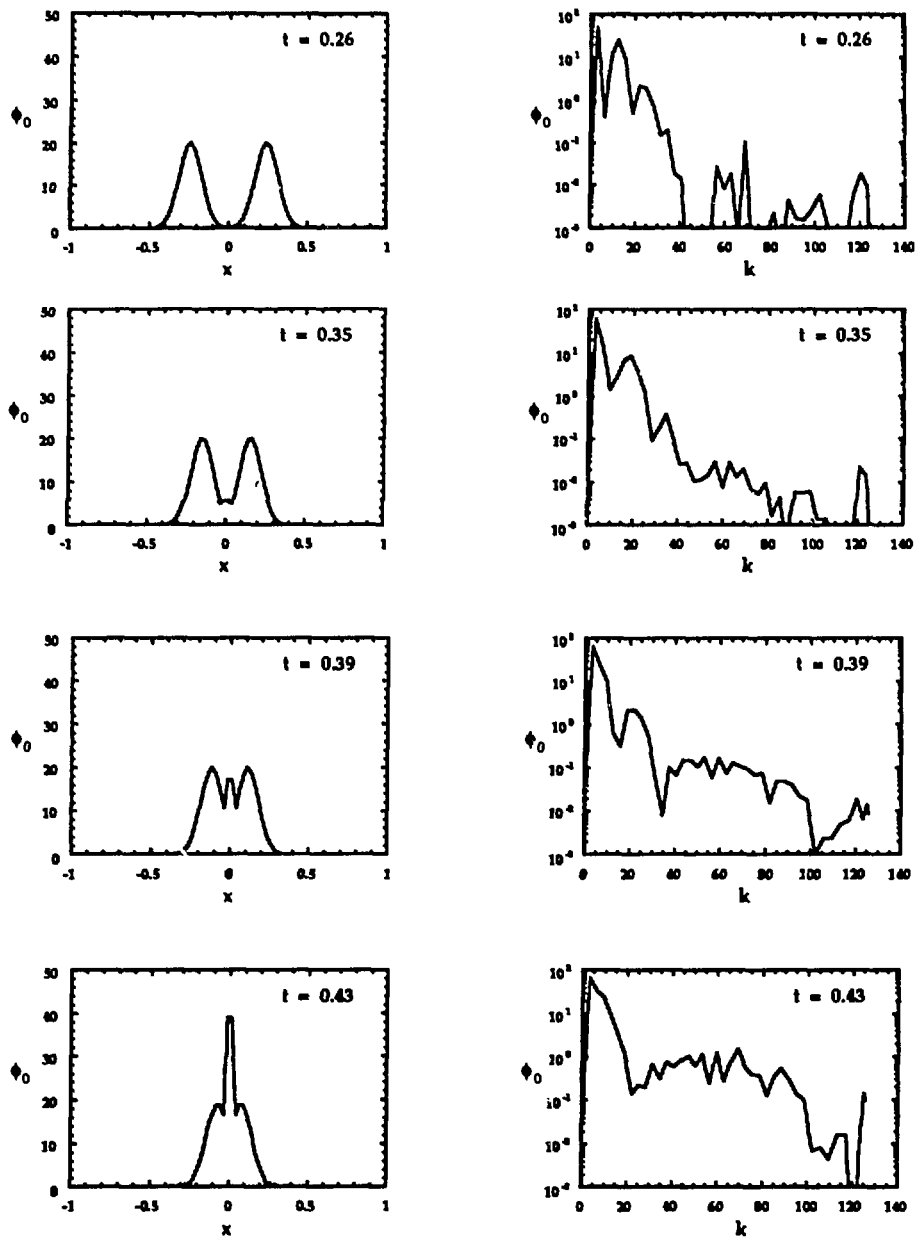


Fig. 7. For case I (80 points, no viscosity), and times  $t = 0.26, 0.35, 0.39$  and  $0.43$ , the left hand frames show  $\phi_0$  as a function of  $x$ , while the right hand frames show its power spectrum as a function of  $k$ .

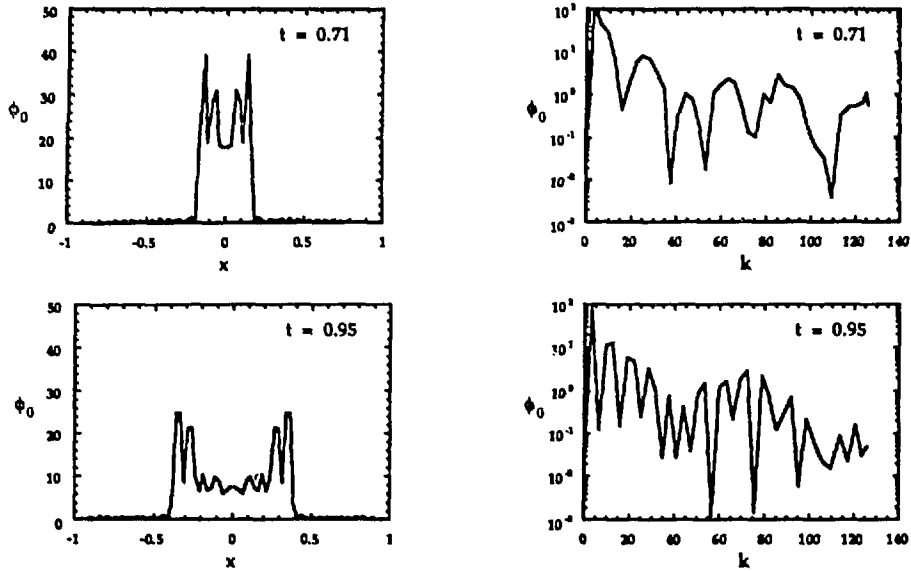


Fig. 8. As Fig. 7, for times  $t = 0.71$  and  $0.95$ .

it is possible to study the effect of random perturbations on  $u$ . The response of  $\phi$  to a Gaussian input in  $u$  at a point in  $x, t$  is shown in Fig. 6. Not only does the response propagate, but it differentiates the input, thus amplifying high-frequency components of the input. If this perturbation is fed back into  $u$  through its nonlinear dependence on  $\phi$ , the higher frequencies are further amplified. The spurious amplitudes can be reduced by introducing an artificial viscosity  $\nu$ , as in the last term on the righthand side of (40). If  $\nu(k_{\max}/2)^2 t_{\max} \sim 5$ , the higher modes are removed without quantitative changes in the solution, other than damping the noise. It should be recalled that the higher frequencies are not propagated correctly in any case.

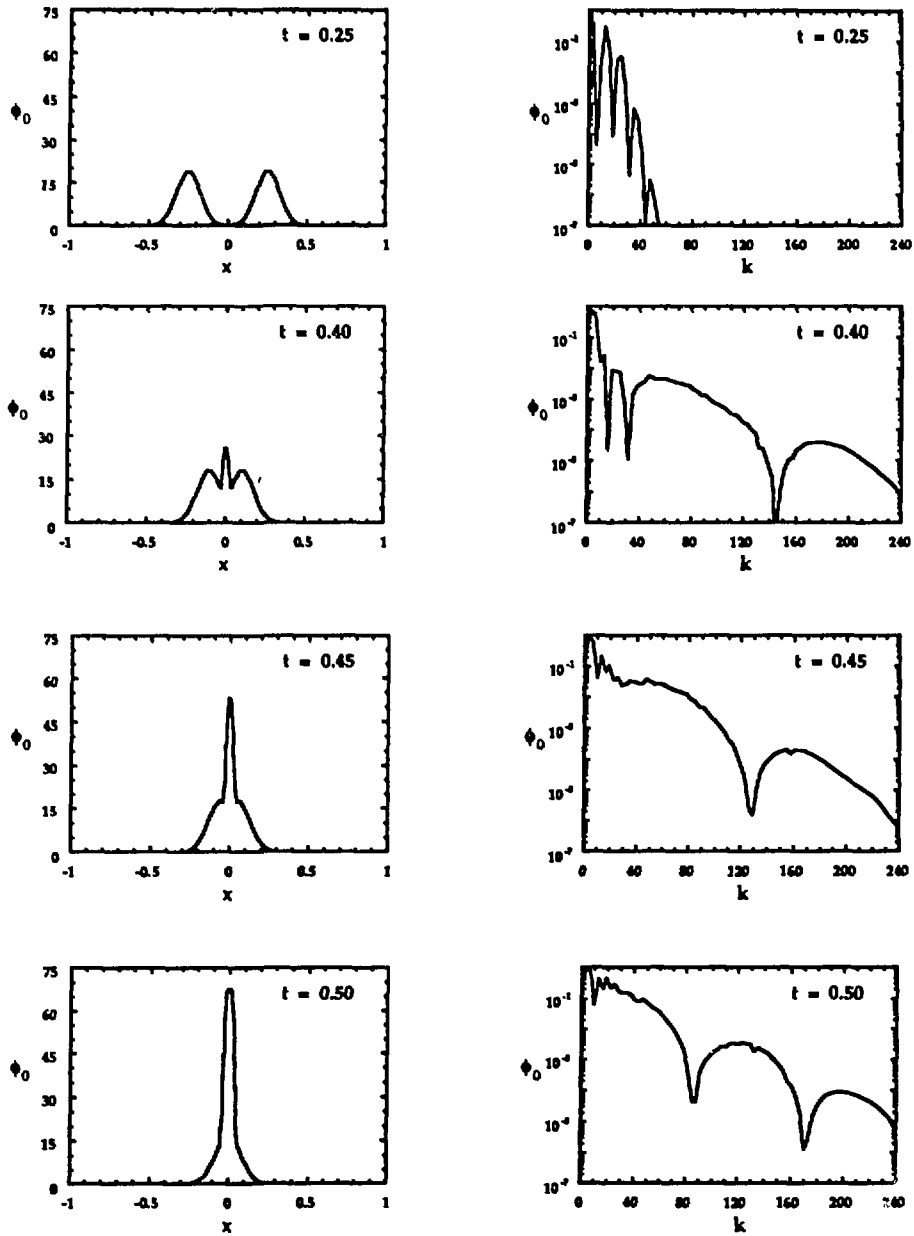


Fig. 9. For case II (160 points, viscosity  $\nu = 10^{-3}$ ), and times  $t = 0.25, 0.40, 0.45$  and  $0.50$ , the left hand frames show  $\phi_0$  as a function of  $x$ , while the right hand frames show its power spectrum as a function of  $k$ .

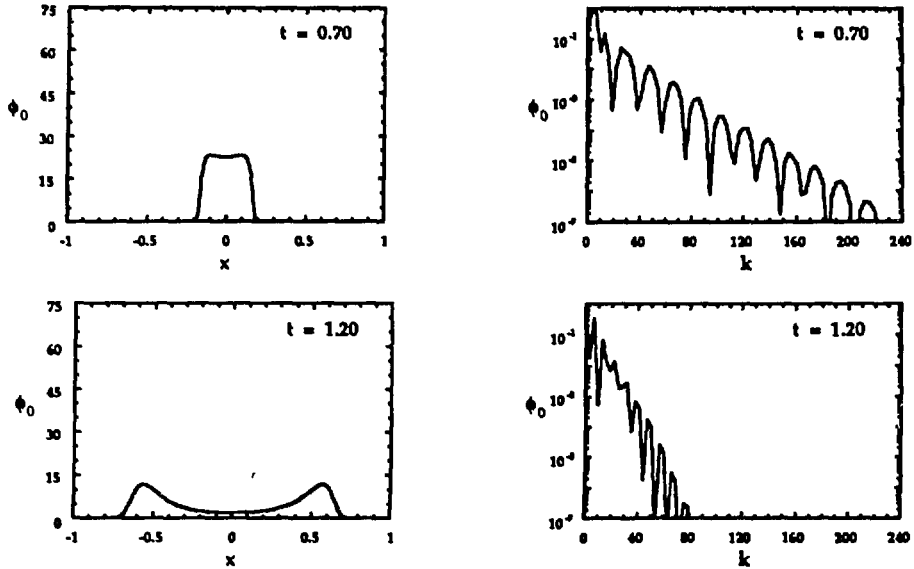


Fig. 10. As Fig. 9, for times  $t = 0.70$  and  $1.20$ .

As a numerical illustration, we present solutions of the system (4), (7) and (8) using 9<sup>th</sup> order splines for a model of two colliding Gaussian drops. In its own rest frame each drop is a Gaussian of unit width and maximum density  $\phi_0 = 0.6$ . The left and right hand drops are boosted toward each other with Lorentz contractions  $\gamma = 10$ , corresponding to 99.5% the speed of light. If length is measured in fermis, and energy in GeV, this model roughly describes two light nuclei colliding at 200 GeV in the frame of one nucleus, an energy presently available at the SPS facility in CERN, Geneva. We show the evolution of  $\phi_0$  and its power spectrum  $A(\phi_0|k)$  for two choices of numerical parameters:

I. No viscosity; 80 points on the interval  $-1 \leq x \leq 1$ . Figures 7 and 8 show  $\phi_0$

and  $A(\phi_0|k)$  side by side.

II. Viscosity  $\nu = 10^{-3}$ ; 160 points on the interval  $-1 \leq x \leq 1$ . Figures 9 and 10 show  $\phi_0$  and  $A(\phi_0|k)$  side by side.

In either case we see the formation of a shock in the middle of the collision, and its subsequent separation into right- and left-moving shocks. In the first case we see the noise appear in the last two time frames; in the power spectrum the higher modes have reached 10% of the physical power. The second case has the same quantitative behaviour, except that the shocks are sharper and the noise is absent. An interesting feature of the power spectrum is the diffraction pattern from the two shock edges!

We conclude that conservation equations can be directly integrated, with good control of most instabilities, using a combination of techniques, notably high order spline bases. Forthcoming papers will discuss the algorithms in greater detail, and present applications to three-dimensional problems.

## 5. ACKNOWLEDGEMENTS

This research was sponsored by the Division of Nuclear Physics, U.S. Department of Energy under contract No. DE-AC05-84OR21400 with Martin Marietta Energy Systems, Inc., and by the Division of Chemical Sciences, Office of Basic Energy Sciences.

## REFERENCES

1. A.R. Gourlay, Proc. Roy. Soc. Lond. **A323**, 219 (1971).
2. C. Bottcher and M.R. Strayer, Ann. Phys. (N.Y.) **175**, 64 (1987).
3. Horace Lamb, *Hydrodynamics*, 6th Edition, (Dover, New York, 1945).
4. L.D. Landau, in *Collected Papers of L.D. Landau*, edited by D. ter Haar (Gordon and Breach, New York, 1965), pp. 569 and 665.
5. G. Gatoff, A.K. Kerman and T. Matsui, Phys. Rev. **D36**, 114 (1987).
6. C. De Boor, *Practical Guide to Splines*, (Springer-Verlag, New York, 1978).
7. G. I. Marchuk, *Methods of Numerical Mathematics*, (Springer-Verlag, New York, 1975). (Springer-Verlag, New York, 1984).
8. A.S. Umar, J.S. Wu, M.R. Strayer and C. Bottcher, J. Comp. Phys., **93**, 426 (1991).
9. C. Bottcher and M.R. Strayer. in *Computational Atomic and Nuclear Physics*, edited by C. Bottcher, M.R. Strayer and J.B. McGroory, (World Scientific, Teaneck NJ, 1990), p. 217.